Acta Polytechnica CTU Proceedings **33**:1–7, 2022
https://doi.org/10.14311/APP.2022.33.0001

Published by the Czech Technical University in Prague

COMPARATIVE FLEXURAL PERFORMANCE OF STEEL FIBRE REINFORCED SELF-COMPACTING CONCRETE (SCFRC) RIBBED SLAB WITH DIFFERENT FIBRE PROVISION AREA

Hazrina Ahmad[a,*], Mohd Hisbany Mohd Hashim[b], Afidah Abu Bakar[b], Fariz Aswan Ahmad Zakwan[a], Ruqayyah Ismail[a]

[a] *Faculty of Civil Engineering, Universiti Teknologi MARA, Cawangan Pulau Pinang, Kampus Permatang Pauh, 13500 Permatang Pauh, Pulau Pinang, Malaysia*

[b] *Faculty of Civil Engineering, Universiti Teknologi MARA, 40450 Shah Alam, Selangor, Malaysia*

[*] corresponding author: hazrina180@uitm.edu.my

Abstract.

The flexural performance of three SCFRC ribbed slabs with different fibre provision area were investigated in this paper; in both ribs and flange (SFWS), ribs only with additional welded mesh in flange (SFT) and in ribs only (SFR). Short hooked end fibres of 35 mm length of 1% volume fraction was blended with the flowable self-compacting concrete (SCC) were used as the material for the slabs. Slab samples of $2.8 \times 1.2 \times 0.2$ m were constructed and loaded until failure under four-point bending. Investigation was carried out in view of the load bearing capacity, deflection, energy absorption capacity as well as the failure modes. The influence of the steel fibre provision on the strain distribution was also examined.

Keywords: Ribbed slab, self-compacting concrete, steel fibres.

1. Introduction

Steel fibre reinforced concrete (SFRC) can be applied in structural slabs that usually cater uniformly distributed low and moderate loads owing to the ability of the steel fibres (SF) to reduce brittleness and enhance its mechanical properties. In consideration of the workability and fibre distribution of the fibre concrete used, this study focuses on the utilization of self-compacting fibre reinforced concrete (SCFRC) that is able to be cast in place without any vibration. The flow ability of the SCFRC offer advantage to the construction process that further leads to a reduction of manpower cost and time [1]. At present, the inclusion of steel fibres is now extended as the main reinforcing material in slab applications to partially or totally replace conventional reinforcements. A number of studies had been performed utilizing SCFRC material in flat slab [2–7]. However, limited studies were found on literatures concerning a ribbed profiled structure. To date, studies on the application of steel fibres in slab structures with rib profile were still limited to its application in normal steel fibre reinforced concrete with low volume fraction (0.5%) [8–10].

The objective of this research is to experimentally determine the ultimate flexural strength, load-deflection curves and the energy absorption capacity of SCFRC ribbed slabs varying in the provision area of the steel fibres (fully and partially steel fibre reinforced).

2. Experimental program

Nine (9) numbers of SCFRC ribbed slabs were cast with 2800 mm length, 1200 mm width and overall thickness of 200 mm. Two ends of the slabs were simply supported on rollers providing clear effective span length of 2600 mm. Two-line loads were applied on the slabs under displacement control of 0.1 mm/sec. Sensitive linear voltage differential transducers (LVDT) were used to measure the displacement at the slab centre (rib and flange soffit).

Grade C30/37 plain self-compacting concrete (PSCC) mix was used for the fabrication of the ribbed slab samples with the mix proportions shown in Table 1. The volume fraction of the hooked end steel fibres was 1% which corresponds to 80 kg/m^3. Detail properties of the steel fibres is shown in Table 2. The mechanical properties of the PSCC and SCFRC mix used in this research is discussed elsewhere [11].

Similar SCC mix was used for the SCFRC mix in combination with the steel fibres. The SCFRC mix was classified as SF1 [12], thus no vibration was applied during casting of the samples. Details on the variation of the slab samples are listed in Table 3 while Figure 1 presents the steel fibre provision in the slab samples applied in this research. The SCFRC ribbed slab are divided into three categories; i.e. full steel fibre reinforced (SFWS), partially steel fibre reinforced with welded mesh (SFT) and partially steel fibre reinforced without welded mesh (SFR). Each type of samples also varies in terms of its topping flange thicknesses (80, 100 and 120 mm).

Cement CEM I 42.5R	Pulverized fly ash	10 mm coarse aggregate	Fine aggregate	Water	w/c	Steel fibre content
315 kg/m^3	105 kg/m^3	830 kg/m^3	865 kg/m^3	185 kg/m^3	0.44	80 kg/m^3

Table 1. SCC mix composition.

Fibre type	Tensile strength (N/mm^2)	Length L (mm)	Diameter d_f (mm)	Fibre aspect ratio L/d_f
Hooked end	1250	35	0.55	65

Table 2. Steel fibre properties.

Reinforcement	Designation		Topping flange thickness (mm)
Fully steel fibre reinforced	SFWS	SFWS80	80
		SFWS100	100
		SFWS120	120
Partially steel fibre reinforced with BRC	SFT	SFT80	80
		SFT100	100
		SFT120	120
Partially steel fibre reinforced without BRC	SFR	SFT80	80
		SFT100	100
		SFT120	120

Table 3. SCFRC sample details.

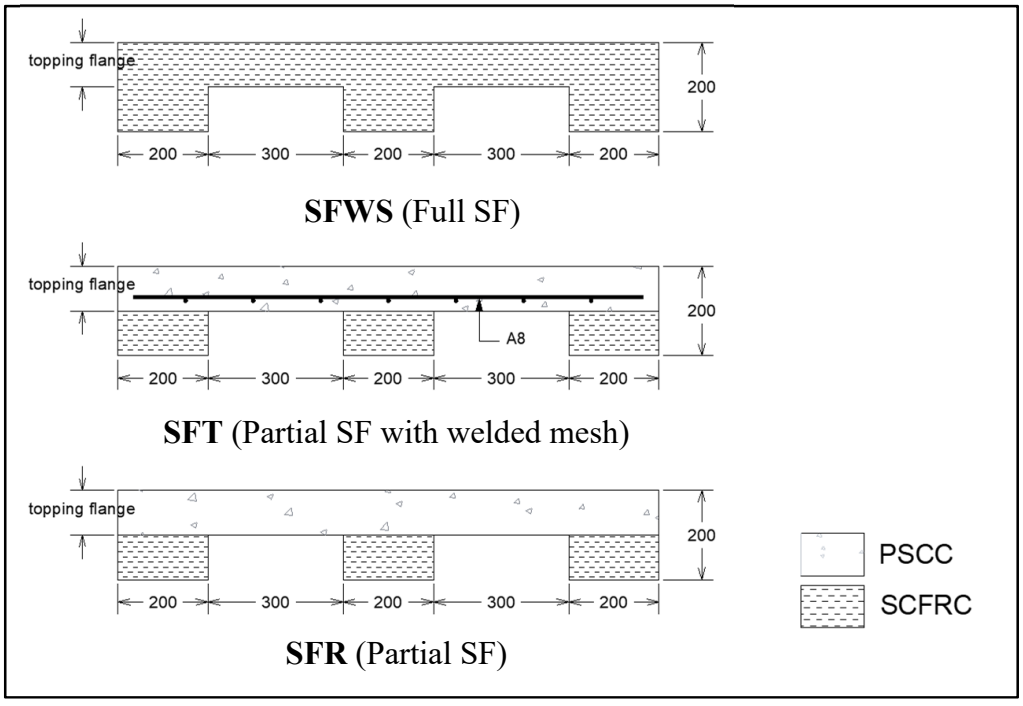

Figure 1. Steel fibre provision area.

Sample	First crack load P_{cr} (kN)	Ultimate load P_{ult} (kN)	Displacement at ultimate load δ_{ult} (mm)	Energy absorption at P_{ult} (kNmm)	Total energy absorption (kNmm)
SFWS80	35.78	57.83	8.75	403.15	1298.91
SFWS100	47.67	60.00	7.8	367.56	1379.22
SFWS120	46.04	74.71	12.47	716.73	1540.65
SFT80	42.89	50.66	3.17	104.23	823.49
SFT100	49.14	51.64	2.97	99.96	1019.92
SFT120	39.53	49.25	7.95	320.01	794.38
SFR80	47.89	55.65	3.17	117.11	482.52
SFR100	44.69	49.3	2.1	66.72	375.83
SFR120	46.26	54.79	2.61	87.46	264.72

TABLE 4. Flexural test results.

3. EXPERIMENTAL RESULTS AND DISCUSSION

3.1. FIRST CRACK AND ULTIMATE STRENGTH OF RIBBED SLABS

The presence of the steel fibres significantly influences the first crack occurrence of the SCFRC ribbed slab. The experimental results of the flexural test are presented in Table 4. The first crack load of all SFWS, SFT and SFR samples were found to be approximately double the first crack load of conventional ribbed slab sample without any steel fibres. The first crack values used for comparison are 17.59, 21.39 and 21.99 kN for 80, 100 and 120 mm flange thickness, respectively. These results are reported elsewhere [13]. Additionally, the first crack load of all samples was observed to be more than 60% of the ultimate load achieved, proving the ability of the steel fibres to transfer stresses across the cracks within the concrete matrix.

Furthermore, the provision of steel fibres also significantly influences the ultimate strength of the ribbed slab that corresponds to the major crack initiation in the ribbed slab samples. The SFWS samples that were fully reinforced with steel fibres achieved the highest ultimate load even with the absence of any conventional reinforcements. Partially reinforced samples (SFT and SFR) however, achieved lower ultimate loads. This might be due to the faster occurrence of the major crack in the sample since the steel fibres were only provided in the ribs causing the stress transfer within the matrix to be more rapid. The presence of the welded mesh in the topping flange also showed no significant contribution to the ultimate strength of the partially steel fibre reinforced samples as it is not in the tension zone.

3.2. LOAD-DISPLACEMENT

The load-displacement curves for all SCFRC ribbed slab samples are shown in Figure 2. Before the first crack occurrence, the elastic region was steeper for the partially SF reinforced samples (SFT and SFR) in comparison to the SFWS samples that showed a more gradual increment. Beyond the first crack occurrence, only the SFWS samples exhibited displacement-hardening response towards the ultimate load displaying the efficiency of the SF to transfer the stresses within the cracked samples.

This hardening behaviour is in relation to the existence of the SF in the topping flange that played an important role in resisting the formation of the cracks as it propagates from the ribs to the flange section. At this point, some of the steel fibres will be subjected to pull-outs as the loading continues. This displacement-hardening response was less significant in the partially SF reinforced samples (SFT and SFR) even with presence of the welded mesh reinforcement in the topping flange.

Beyond the ultimate load, all samples experienced displacement-softening response where the load carrying capacity gradually decrease as the vertical displacement continues to increase further. Gradual softening curves are exhibited by the SFWS and SFT samples reaching up to 32 mm displacement. In contrast, the SFR samples underwent more abrupt softening resulting lower displacement reflecting to a more brittle behaviour of the structure.

In view of the topping flange thickness for each type of samples, the increase in the topping flange thickness significantly affects the softening curves. Steeper curves were observed for 120 mm topping flange thicknesses of all ribbed slab samples exhibiting a more brittle post-cracking behaviour as the topping thickness increases beyond half of the total slab depth (100 mm). This brittleness might be as the result of the topping thickness that enters the tensile zone of the sample reducing the function of the rib section. This finding also agrees well with the previous findings where higher slab thickness resulted in higher brittleness of the section [3, 14].

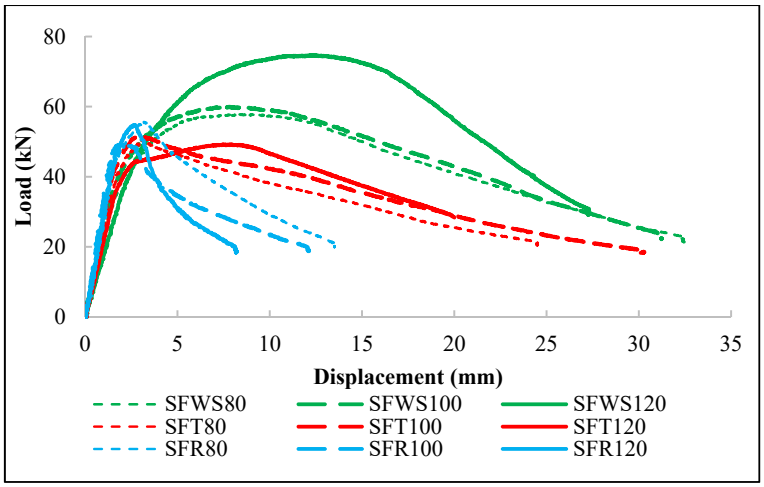

Figure 2. Load-displacement curves.

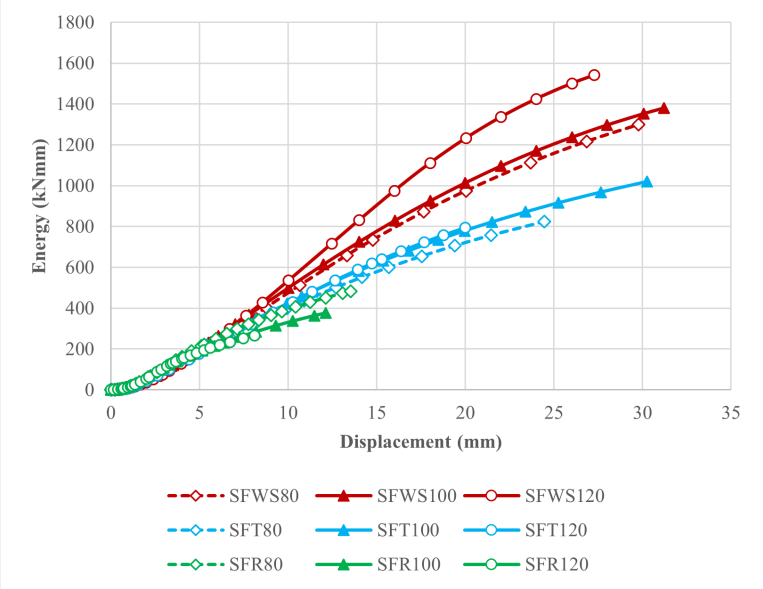

Figure 3. Energy absorption capacity.

3.3. Vertical displacement

At ultimate load, the highest displacement was exhibited by the SFWS samples at both ultimate load and at final failure of the samples (Table 4). This was followed by the SFT and SFR samples. The SFR samples which are more brittle experienced the lowest vertical displacement at ultimate load as well as at final failure exhibiting a lower level of ductility. Nevertheless, all samples fulfilled the displacement requirement at service load whereas the values are within the allowable limit (L/500) as stated in the Eurocode 2 revealing the capability of the SCFRC samples under flexural load.

In view of the topping flange thickness, the lowest displacement at ultimate load was observed in the samples with 100 mm topping flange thickness for all types of samples. This can be related to the location of the neutral axis and the transmission of the stresses between the rib and flange section of the ribbed slab. At final failure, however, the 120 mm samples experienced the lowest displacement that is as the result of the brittle behaviour of the SCFRC ribbed slab as the topping flange thickness increases.

3.4. Energy absorption capacity

Steel fibre inclusion enhances the energy absorption capacity of the slab as calculated by the area under the load-displacement curve. Higher volume of steel fibres in concrete resulted in an increase in the energy absorbed by the slab structure. The SFWS samples showed the highest energy absorption capacity at the ultimate load as well as the total energy (see Table 4).

The energy absorption capacity is in close relation with the total volume of SF in the slab. The SFWS samples showed higher energy absorption for higher flange thicknesses. However, a contradict trend were observed in the SFT and SFR samples showing the relation towards the provision area of the SF (Figure 3).

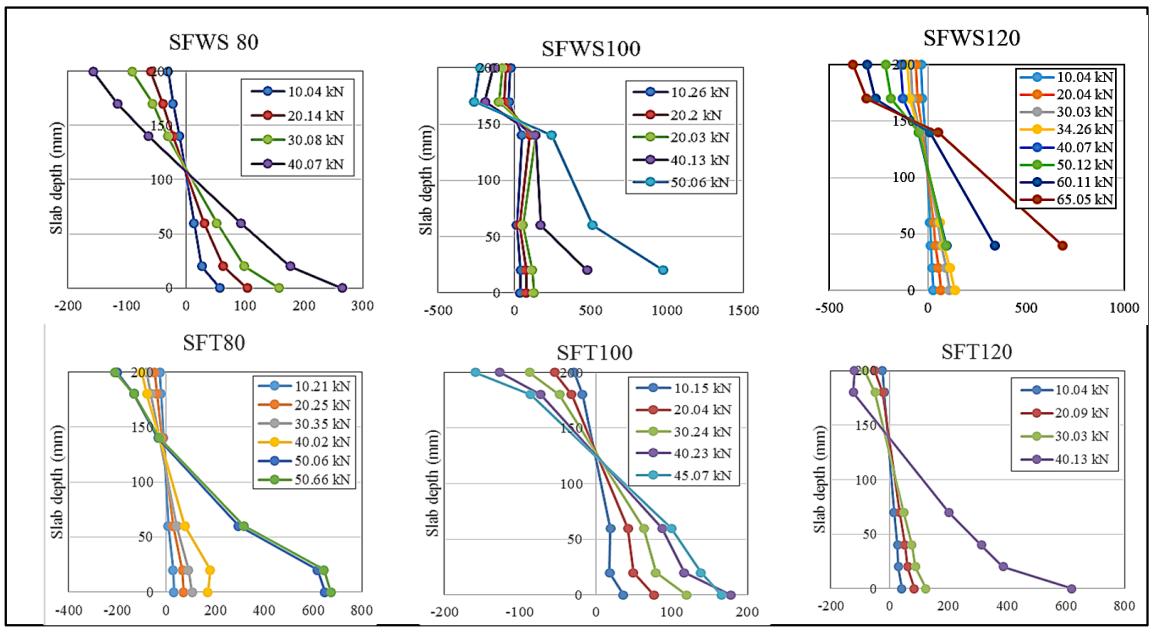

FIGURE 4. Strain distribution of SFWS and SFT samples.

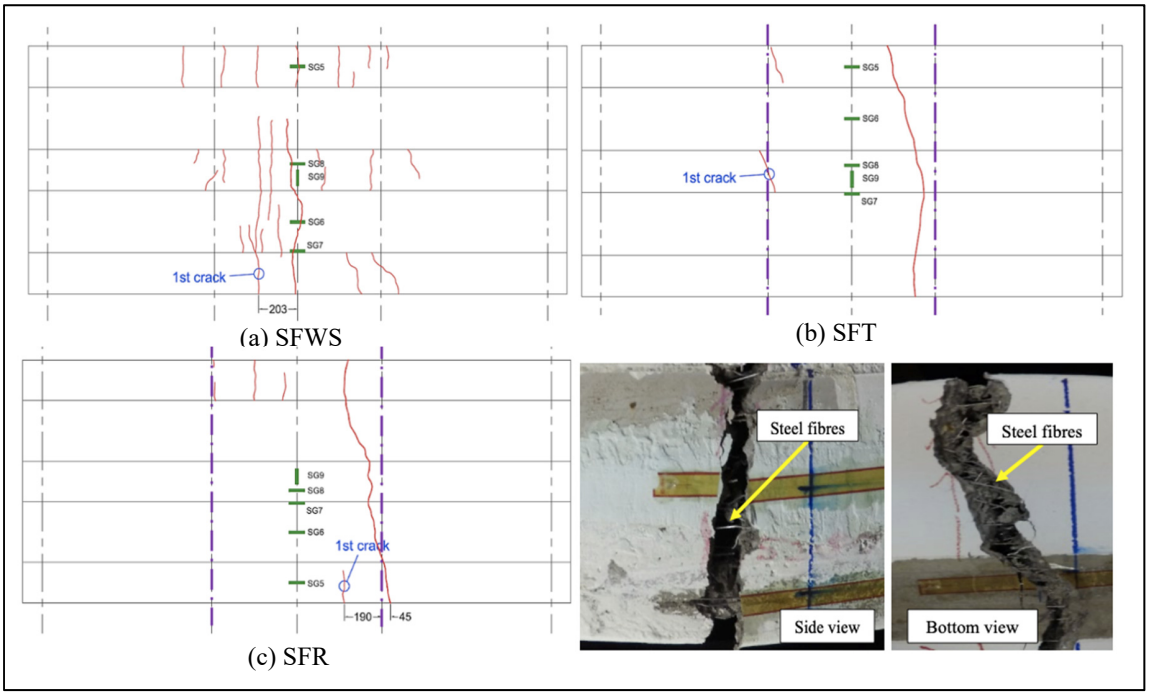

FIGURE 5. Crack pattern of the SCFRC ribbed slab and steel fibres bridging the cracks.

3.5. STRAIN DISTRIBUTION

The neutral axis location of the SCFRC ribbed slab samples can be determined based on the strain distribution across the depth of the slab at various stages of loading. For the SFWS samples, only for 80 mm topping thickness, the neutral axis falls below the topping flange. The neutral axis falls in flange for all other samples, including all SFT and SFR samples. No significant effect of the topping flange on the neutral axis location thickness was observed. The strain distribution for the SCFRC ribbed slab samples is presented in Figure 4.

The view of the bridging steel fibres is also presented in Figure 5. From the crack openings, it can be observed that most of the steel fibres were in the longitudinal direction that is perpendicular to the crack direction. The steel fibres had effectively bridged the cracks by holding the matrix together and the hooked end shape had assisted in increasing the bonding to the concrete matrix contributing to the structural strength to resist loads.

The crack pattern for the partially reinforced samples (SFT and SFR) were different from the SFWS samples whereas it only experienced one major crack

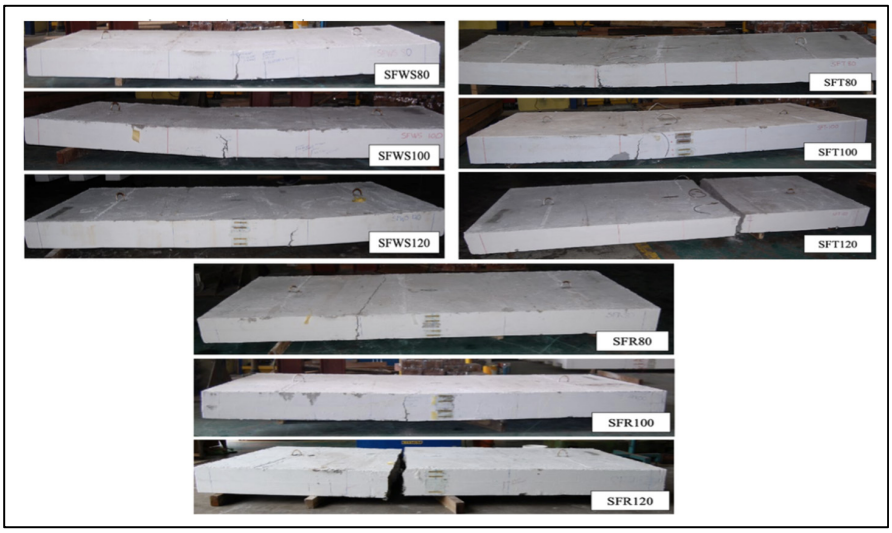

Figure 6. SCFRC ribbed slab at final failure.

line with very minimal minor cracks across the sample. The crack started at the rib's soffit and propagated to the flange soffit. The SFT samples underwent ductile failure, gradually failing after the ultimate load was reached. The SFR samples on the other hand experienced a more rapid crack propagation experiencing a more brittle failure.

3.6. Crack pattern and failure modes

Figure 5 showed the crack pattern of the SFWS samples. The first crack of all three SFWS samples was detected within the central region of the ribbed slab located at the external rib soffit.

After the occurrence of the first crack, more cracks developed at the external rib's soffit on both sides of the sample as well at the middle rib soffit. These cracks then continued to propagate to the sides of the rib sections and further to the soffit of the flange as the loading continued. As the cracks continued to widen at the ribs, it could be visually observed from the slow propagating cracks that the steel fibres had effectively bridged the cracks as the loading continued to increase further.

The view of the bridging steel fibres is also presented in Figure 5. From the crack openings, it can be observed that most of the steel fibres were in the longitudinal direction that is perpendicular to the crack direction. The steel fibres had effectively bridged the cracks by holding the matrix together and the hooked end shape had assisted in increasing the bonding to the concrete matrix contributing to the structural strength to resist loads.

The crack pattern for the partially reinforced samples (SFT and SFR) were different from the SFWS samples whereas it only experienced one major crack line with very minimal minor cracks across the sample. The crack started at the rib's soffit and propagated to the flange soffit. The SFT samples underwent ductile failure, gradually failing after the ultimate load was reached. The SFR samples on the other hand experienced a more rapid crack propagation experiencing a more brittle failure.

In view of the topping thickness variation, the cracks were observed to be more concentrated on the rib soffit of the SFWS samples with lower flange thicknesses (80 mm and 100 mm). Consequently, more cracks were observed to be distributed over the flange soffit for the 120 mm topping thickness.

At the end of the loading test, all SFWS samples still remained intact, held by the steel fibres in the ribs and topping flange (Figure 6). As for the SFT and SFR samples, all samples except for the samples with 120 mm topping thickness remains intact at final failure with the assistance of the welded mesh and bridging of the fibres in the ribs section. Samples with 120 mm thickness experienced brittle failure, i.e. breaking into two at the end of the loading process. These conditions might be due to the reduced thickness of the rib section resulting smaller volume of the steel fibres to bridge the cracks.

4. Conclusion

Based on the results, these conclusions can be drawn:

1. All SCFRC ribbed slab underwent flexural failure. The fully SF reinforced samples experienced multiple cracks while the partially SF reinforced samples experienced only one major crack, displaying the significant effect of the steel fibre provision under flexural load.
2. The fully SF reinforced samples also achieved the highest ultimate load at higher deflection exhibiting higher level of ductility amongst all samples
3. Increase in the flange thickness resulted an increase in the ultimate load for the SFWS samples but shows no significant increase in the SFT samples. Beyond the ultimate load, samples with higher

flange thickness becomes more brittle resulting in a more rapid strength loss.

Overall, based on the experimental results, it can be concluded that the fully steel fibre reinforced sample (SFWS) with the highest flange thickness displayed a good performance under bending.

Acknowledgements

Special thanks to the laboratory staffs of the Faculty of Civil Engineering, Universiti Teknologi MARA for their technical support and the Institute of Research Management and Innovation (IRMI), UiTM for their assistance in managing the research process. This study was funded by the E-science Fund (06-01-01-SF0835) from the Ministry of Science, Technology and Innovation (MOSTI) of Malaysia.

References

[1] M. Pająk, T. Ponikiewski. Flexural behavior of self-compacting concrete reinforced with different types of steel fibers. *Construction and Building Materials* **47**:397-408, 2013. https://doi.org/10.1016/j.conbuildmat.2013.05.072.

[2] A. Blanco, P. Pujadas, A. de la Fuente, et al. Assessment of the fibre orientation factor in SFRC slabs. *Composites Part B: Engineering* **68**:343-54, 2015. https://doi.org/10.1016/j.compositesb.2014.09.001.

[3] J. Michels, D. Waldmann, S. Maas, et al. Steel fibers as only reinforcement for flat slab construction - Experimental investigation and design. *Construction and Building Materials* **26**(1):145-55, 2012. https://doi.org/10.1016/j.conbuildmat.2011.06.004.

[4] Steel Fiber Concrete Slabs on Ground: A Structural Matter. *ACI Structural Journal* **103**(4), 2006. https://doi.org/10.14359/16431.

[5] H. Salehian, J. A. O. Barros. Assessment of the performance of steel fibre reinforced self-compacting concrete in elevated slabs. *Cement and Concrete Composites* **55**:268-80, 2015. https://doi.org/10.1016/j.cemconcomp.2014.09.016.

[6] K. S. Regab, Study Punching Shear of Steel Fiber Reinforced Self Compacting Concrete Slabs by Nonlinear Analysis, *International Journal of Civil, Environmental, Structural, Construction and Architectural Engineering*, **7**(9):624-635, 2013.

[7] M. D. E. Teixeira, J. A. O. Barros, V. M. C. F. Cunha, et al. Numerical simulation of the punching shear behaviour of self-compacting fibre reinforced flat slabs. *Construction and Building Materials* **74**:25-36, 2015. https://doi.org/10.1016/j.conbuildmat.2014.10.003.

[8] A. S. Samsudin, Structural Performance of Steel Fibre Reinforced Concrete Ribbed Slab Panel, Universiti Teknologi MARA, 2018.

[9] F. A. Rahman, A. A. Bakar, M. H. M. Hashim, et al. Flexural performance of steel fiber reinforced concrete (SFRC) ribbed slab with various topping thicknesses. 2017. https://doi.org/10.1063/1.5011493.

[10] M. H. Mohd Hashim, S. H. Hamzah, H. Ahmad, et al. Preliminary Investigation on the Flexural Behaviour of Steel Fibre Reinforced Self-Compacting Concrete Ribbed Slab. *Scientific Research Journal* **15**(1), 2018. https://doi.org/10.24191/srj.v15i1.4166.

[11] A. Hazrina, M. H. Mohd Hisbany, A. B. Afidah, et al. Effects of Steel Fibre Addition on the Mechanical Properties of Steel Fibre Reinforced Self-Compacting Concrete (Sccfibre). *IOP Conference Series: Materials Science and Engineering* **431**, 2018. https://doi.org/10.1088/1757-899x/431/4/042004.

[12] The European Guidelines for Self-Compacting Concrete, no. May. European Project Group, 2005.

[13] H. Ahmad, M. H. M. Hashim, A. A. Bakar, et al. Flexural performance of full and partially steel fibre reinforced self-compacting concrete (SCFRC) ribbed slab. I*OP Conference Series: Materials Science and Engineering* **615**(1), 2019. https://doi.org/10.1088/1757-899x/615/1/012094.

[14] L. Facconi, F. Minelli. Verification of structural elements made of FRC only: A critical discussion and proposal of a novel analytical method. *Engineering Structures* **131**:530-41, 2017. https://doi.org/10.1016/j.engstruct.2016.10.034.